Citation for published version:
Mahmoudi, H, Bagherzadeh, M, Ataie, S, Kia, R, Heydar Moravej, S, Zare, M, Raithby, PR, Ferlin, F & Vaccaro, L 2020, 'Synthesis and X-ray crystal structure of a Molybdenum(VI) Schiff base complex: Design of a new catalytic system for sustainable olefin epoxidation', *Inorganica Chimica Acta*, vol. 511, 119775. https://doi.org/10.1016/j.ica.2020.119775

DOI:
10.1016/j.ica.2020.119775

Publication date:
2020

Document Version
Peer reviewed version

Link to publication

Publisher Rights
CC BY-NC-ND

University of Bath

Alternative formats
If you require this document in an alternative format, please contact:
openaccess@bath.ac.uk

General rights
Copyright and moral rights for the publications made accessible in the public portal are retained by the authors and/or other copyright owners and it is a condition of accessing publications that users recognise and abide by the legal requirements associated with these rights.

Take down policy
If you believe that this document breaches copyright please contact us providing details, and we will remove access to the work immediately and investigate your claim.

Download date: 29. May. 2023

Synthesis and X-ray Crystal Structure of a Molybdenum(VI) Schiff Base Complex: Design of a New Catalytic System for Sustainable Olefin Epoxidation

Hamed Mahmoudi,[a] Mojtaba Bagherzadeh,[a*] Saeed Ataie,[a] Reza Kia,[a] Seyed Heydar Moravej,[a] Maryam Zare[b], Paul R. Raithby[c], Francesco Ferlin[d] and Luigi Vaccaro[d]

[a] *Chemistry Department, Sharif University of Technology, Tehran, P.O. Box 11155-3615, Iran; bagherzadeh@sharif.edu*

[b] *Department of Basic Sciences, Golpayegan University of Technology, PO Box 87717-65651, Golpayegan, Iran*

[c] *Department of Chemistry, University of Bath, Bath BA2 7AY, UK*

[d] *Laboratory of Green S.O.C. – Dipartimento di Chimica, biologia e Biotecnologie, Università degli Studi di Perugia, Via Elce di Sotto 8, 06123 – Perugia, Italy.*

Abstract: A targeted new dioxo molybdenum(VI) ONO Schiff base complex was prepared for catalyzing epoxidation of olefins in water. This complex was characterized by FT-IR, NMR, UV-Vis, and X-ray crystallography techniques. DFT calculations are additionally performed to find ground and transition states for finding electronic structure and UV-Vis assignment. Afterward, a new protocol was defined for sustainable catalytic epoxidation of olefin in water using this complex as a green catalyst, and also remarkable results are obtained, such as turn over number up to 1400.

Keywords: **Mo(VI) Schiff base, Crystal Structure, Epoxidation in Water, Sustainable Catalysis, DFT Study**

1. INTRODUCTION

Epoxidation is a fundamental chemical process for the transformation of olefins into fine chemical products, which is fundamental to several industrial applications and for the preparation of complex molecules such as pharmaceutical compounds[1]. The constant high interest in the epoxidation process is confirmed by numerous publications in the field [2]. Early transition metals, containing high oxidation states such as Mo(VI), V(V), Re(VII) and W(VI), are able to catalyze epoxidation of olefins effectively [3], and among these high-valent metals, molybdenum is very effective [4]. There are various examples of molybdenum(VI), used as catalysts in industry, as in the Halcon and Arco processes where homogeneous Mo(VI) catalysts are used for industrial epoxidation of olefins [5].

Molybdenum(VI) Schiff base complexes containing a *cis*-MoO_2 unit, behave like enzymes such as xanthine oxidase and nitrogenase which have active sites containing molybdenum. Endowed with the Mo=O unit, these complexes are employed as catalysts in industry for oxygen atom transfer reactions [6]. The use of metal-organic complexes of Mo(VI) with Schiff base ligands has been reported in many electrochemical applications and biological modeling, as antioxidant and antibacterial factors, and also as catalysts for the production of hydrogen, sulfide oxidations and

alkene epoxidations [7]. In order to emulate biological systems, a lot of dioxo molybdenum(VI) complexes are synthesized and specified so far [6e, 6f, 8].

Over the past few decades, sustainability principles have been adopted by chemical industry [9]. In term of green chemistry, the utilization of environmentally friendly and efficient solvents in organic reactions has led to a new chemistry and evident economic benefits [10]. Water, due to its safety can be a green alternative, in comparison with classic organic solvents, for a less harmful organic synthesis [11].

Design and synthesis of catalytic systems that show high activity in water, has attracted great attention [12]. Due to electronic structures and spatial effects that ligands can provide around a central metal, synthesis and utilization of an efficient ligand can transfer unique properties to a catalytic system, including solubility and high efficiency in water [13]. On the other hand, despite the fact that there is much interest in preparing epoxidation catalytic systems, active in water, few works have been published in this area [3i, 12a-c, 14]. In the best of our knowledge, very few examples of epoxidation in water, catalyzed by dioxo molybdenum(VI) Schiff base complex, have been published so far [4c].

In this work, a new dioxo molybdenum(VI) complex, chelated by a new Schiff-base ligand, has been synthesized and fully characterized. Furthermore, catalytic activity of this complex in epoxidation of olefins was studied in water as a green solvent, and remarkable catalytic potential has been presented for this catalytic system. In this protocol, water was replaced with traditional epoxidation solvent, 1,2-dichloroethane, to reduce toxicity of this toxic solvent to environment. As well as, theoretical studies have been conducted in order to obtain optimum geometrical parameters for this molybdenum complex.

2. EXPERIMENTAL

2.1. Materials and Methods

5-(chloromethyl)-2-hydroxybenzaldehyde [15] (**1**) was prepared according to a modified, previously published procedure. (3-formyl-4-hydroxy-5-methylbenzyl) triphenyl phosphonium chloride [16] (**2**) and bis(acetylacetonato)dioxo molybdenum(VI) [17] (**3**) were synthesized according to the known literature methods. Acetylacetone was purchased from Fluka and it was purified by the previously published method [18]. All other chemicals and solvents were purchased from Merck and Sigma-Aldrich companies and were used as obtained from commercial sources, without further purification. Elemental analyses for carbon, hydrogen, and nitrogen (CHN) were performed on a leco truspec elemental analyzer. FT-IR spectra were obtained employing KBr pellets on a Bruker Tensor 27 FT-IR spectrophotometer. The electronic spectra were recorded in ethanol on a Varian Cary 100 Spectrophotometer. The NMR spectra were recorded at room temperature with a Bruker FT-NMR 500 MHz (^{1}H at 500 MHz, ^{13}C at 125.8 MHz) or Bruker FT-NMR 400 MHz (^{1}H at 400 MHz, ^{13}C at 100.6 MHz and ^{31}P at 162 MHz) spectrometer in $CDCl_3$, DMSO-d_6, and methanol-d_4. Analyzing ^{1}H NMR spectrum was performed using a previously

published method.[19] The catalytic reactions' products were characterized applying an Agilent Technologies 6890 N gas chromatography, equipped with a 19091J-236 HP-5, 5% phenyl methyl siloxane capillary column. Precise temperature adjustment (for the synthesis of 5-(chloromethyl)-2-hydroxybenzaldehyde) was conducted by a WiseCircu WCR-P8 precision refrigerated bath.

2.2. Synthesis of Complex 4

A 100 mL two-neck round bottom flask equipped with a magnetic stirrer and condenser was charged with (3-formyl-4-hydroxy-5-methylbenzyl) triphenylphosphonium chloride (0.866 g, 2 mmol) in 20 mL of ethanol. The mixture was heated up to reflux and 2-aminophenol (0.218 g, 2 mmol) in 20 mL of ethanol was added dropwise over 20 min. The reaction was maintained refluxing for 3 h. After that, an ethanolic solution of bis(acetylacetonato)dioxo molybdenum(VI) (0.652 g, 2 mmol in 20 mL) was poured into the mentioned solution. The reaction mixture was left refluxing and stirring in the air atmosphere for 5 h. After the reaction was completed, the volume of solution was reduced to 10 mL. Then, 20 mL of diethyl ether was added to the solution and resulted red-orange solid was collected by filtration and washed with diethyl ether. (0.988 g, 75% yield). **Anal. Calc. for $Mo_2O_9N_2Cl_2P_2C_{64}H_{52}$:** C 58.33, H 3.98, N 2.13%. found: C 58.47, H 3.91, N 2.11%., **^{1}H NMR (400 MHz, methanol-d_4) δ** = 8.90 (s, 1H), 7.92 – 7.82 (m, 3H), 7.75 – 7.66 (m, 12H), 7.65 (dd, J=8.1, 1.1, 1H), 7.40 (t, J=2.5, 1H), 7.25 (ddd, J=8.2, 7.3, 1.1, 1H), 7.00 (dt, J=8.6, 2.2, 1H), 6.94 (ddd, J=8.1, 7.3, 1.0, 1H), 6.85 (dd, J=8.2, 1.0, 1H), 6.72 (d, J=8.6, 1H), 4.91 (d, J=14.3, 2H).**^{13}C NMR (100.6 MHz, methanol-d_4) δ** = 163.6 (d, J=3.2), 161.9 (s), 156.8 (s), 138.4 (d, J=5.9), 138.4 (d, J=4.1), 136.7 (s), 136.5 (d, J=3.0), 135.4 (d, J=9.7), 131.8 (s), 131.5 (d, J=12.5), 123.8 (d, J=2.9), 122.3 (s), 121.1 (d, J=8.5), 120.7 (d, J=2.8), 118.9 (d, J=85.9), 118.6 (s), 117.0 (s), 29.7 (d, J=48.1). **^{31}P NMR (162 MHz, methanol-d_4) δ** = 22.6 (s). IR (KBr) (νmax/cm^{-1}): 1612 ν(C=N), 900 and 845 ν(Mo=O).

2.3. Crystal structure determination

Single crystals of the complex, suitable for X-ray diffraction analysis, were grown by slow vapor diffusion of diethyl ether into ethanol solution. X-ray intensity data were collected using the full sphere routine by φ and ω scans strategy on the Agilent SuperNova dual wavelength EoS S2 diffractometer with mirror monochromated Cu Kα radiation (λ = 1.54184 Å). For all data collections, the crystals were cooled to 150 K using an Oxford diffraction Cryojet low-temperature attachment. The data reduction, including an empirical absorption correction using spherical harmonics, implemented in SCALE3 ABSPACK scaling algorithm [20], was performed using the CrysAlisPro software package [21]. The crystal structures were solved by direct methods, employing the online version of AutoChem 2.0 [22] in conjunction with OLEX2 [23] suite of programs implemented in the CrysAlis software, and then refined by full-matrix least-squares (SHELXL2014) on F2 [23]. The non-hydrogen atoms were refined anisotropically. Carbon-bound hydrogen atoms were positioned geometrically in idealized positions and refined with the riding model approximation, with Uiso(H) = 1.2 or 1.5 Ueq(C). The oxygen-bound hydrogen atoms were located from the difference Fourier map and constrained to refine with the parent atom. The

program SHELXTL was used for the molecular graphics [23]. All geometric calculations were carried out applying PLATON software [24]. There are two independent molecules in the unit cell. For one molecule the Mo, the axial and equatorial oxo groups and chlorido ligand in MoNO4Cl unit are disordered over two positions, in the ratio 0.814(4):0.186(4). For the first compound, the two components of one oxo oxygen and the Cl atom were assigned the same position, while the two components of Mo atoms and of one oxo atom were assigned the same anisotropic displacement parameters. For the second molecule, the triphenylphosphine group was distributed over two positions, by rotation around the P—C bond; both components were restrained to have the same geometry while all carbon atoms were restrained to have similar anisotropic displacement parameters. The final ratio of the two components were 0.559(7):0.441(7). The difference map showed a number of peaks, due to disordered diffuse solvent. The contribution to the solvent was treated with the SQUEEZE routine of PLATON, the unit cell contained 6 cavities each of which was consistent with the presence of 7 molecules of water per cavity (per cavity unit).

2.4. General procedure for catalytic epoxidation in water

In a 5 mL round bottom flask equipped with condenser and magnetic stirrer, complex **4** as catalyst (0.0013 g, 0.002 mmol), olefin (1 mmol), water (0.5 mL) and TBHP-H_2O (tert-butyl hydrogen peroxide, 70% in water, 2 mmol, 274 µL) were added and the resulting mixture was left under stirring at 80 °C under atmospheric pressure. After 5 h the product was extracted using ethyl acetate (2 mL) and dried using sodium sulfate. The reaction progress was monitored by GLC (Gas-Liquid Chromatography) system and the conversions and epoxide selectivity were calculated using chromatographic peak integration (n-octane (1mmol, 163 µL) was used as internal standard). The products were identified by standard samples.

3. RESULTS AND DISCUSSION

3.1. Synthesis and characterization

1, **2** and **3** have been synthesized through a routine procedure and characterized by NMR spectroscopy (see supporting information for more details). **4** has been synthesized by addition of **3** to refluxing ethanolic mixture of **2** and 2-aminophenol (Fig. 1).

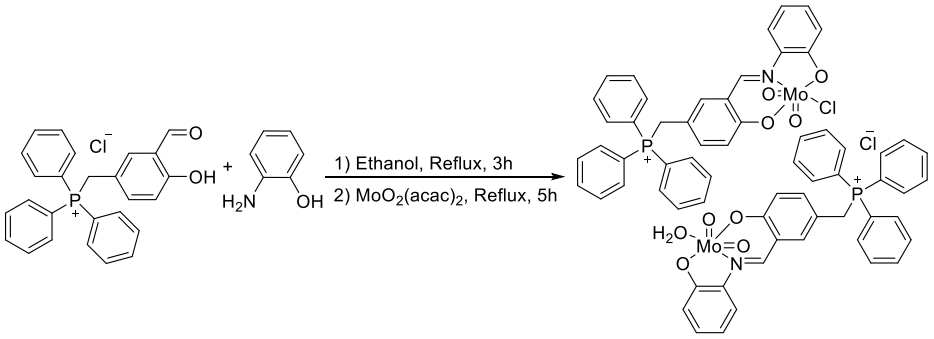

Figure 1. Synthesis of complex **4**

^{1}H NMR spectrum of **4** (Fig. S8, supporting information) shows a singlet resonance at δ=8.90 ppm, which was designated to the aldimine hydrogen atom. Three sets of multiple resonances between δ=7.66-7.92 ppm were allocated to hydrogen atoms of phenyl phosphonium rings. The signal between δ=7.82-7.92 ppm can be allocated to para-hydrogen atoms of phenyl phosphonium rings, and also the pattern of this resonance looks like an incomplete doublet of the triplet, due to the long-range coupling of these hydrogen atoms with phosphor atom and other hydrogen atoms, which makes it difficult to analyze. The resonance of hydrogen atoms of Meta and Ortho positions of phenyl phosphonium rings were appeared at δ=7.71-7.75 ppm and δ=7.65-7.71 ppm respectively, and they were also merged together. These three sets of resonances are correlated together, as shown in the ^{1}H-^{1}H COSY NMR spectrum (Fig. S12 and S13). The analysis of coupling between hydrogen atoms of the benzyl ring and iminophenol ring is shown in Fig. 2. According to Fig. 2, two sets of the doublet of doublet pattern can be observed at δ= 7.65 and δ= 6.85 ppm and they were assigned to hydrogen atoms of ((h)) and ((c)) respectively. Other two sets of resonances with a doublet of the doublet of doublet pattern at δ= 7.25 and δ= 6.94 ppm can be assigned to hydrogen atoms of ((f)) and ((d)) respectively. The hydrogen atoms of ((c)), ((d)), ((f)) and ((h)) are correlated together, as observed in ^{1}H-^{1}H COSY NMR spectrum (Fig. S12 and S13). The resonances of hydrogen atoms of ((b)) and ((e)) were appeared at δ= 6.72 and δ= 7.00 ppm respectively. These two hydrogen atoms are correlated together and they split each other into doublet signals. In addition, the hydrogen atom ((b)) has a long-range coupling with benzyl hydrogen with $^{4}J_{HH}$=2.2 Hz, which justifies why it shows a triplet of doublet pattern. Another signal at δ= 7.40 ppm was related to hydrogen atom ((g)) that displays the triplet pattern because of correlation with benzylic hydrogen with $^{4}J_{HH}$=2.5 Hz. Finally, the resonance of benzylic hydrogen atoms was appeared at δ=4.91 ppm which has a doublet pattern with $^{2}J_{PH}$=14.3 Hz. The broadening of benzylic hydrogen resonance is due to further coupling with ((g)) and ((e)) hydrogen atoms with constant coupling $^{4}J_{HH}$=2.5 and 2.2 Hz, respectively.

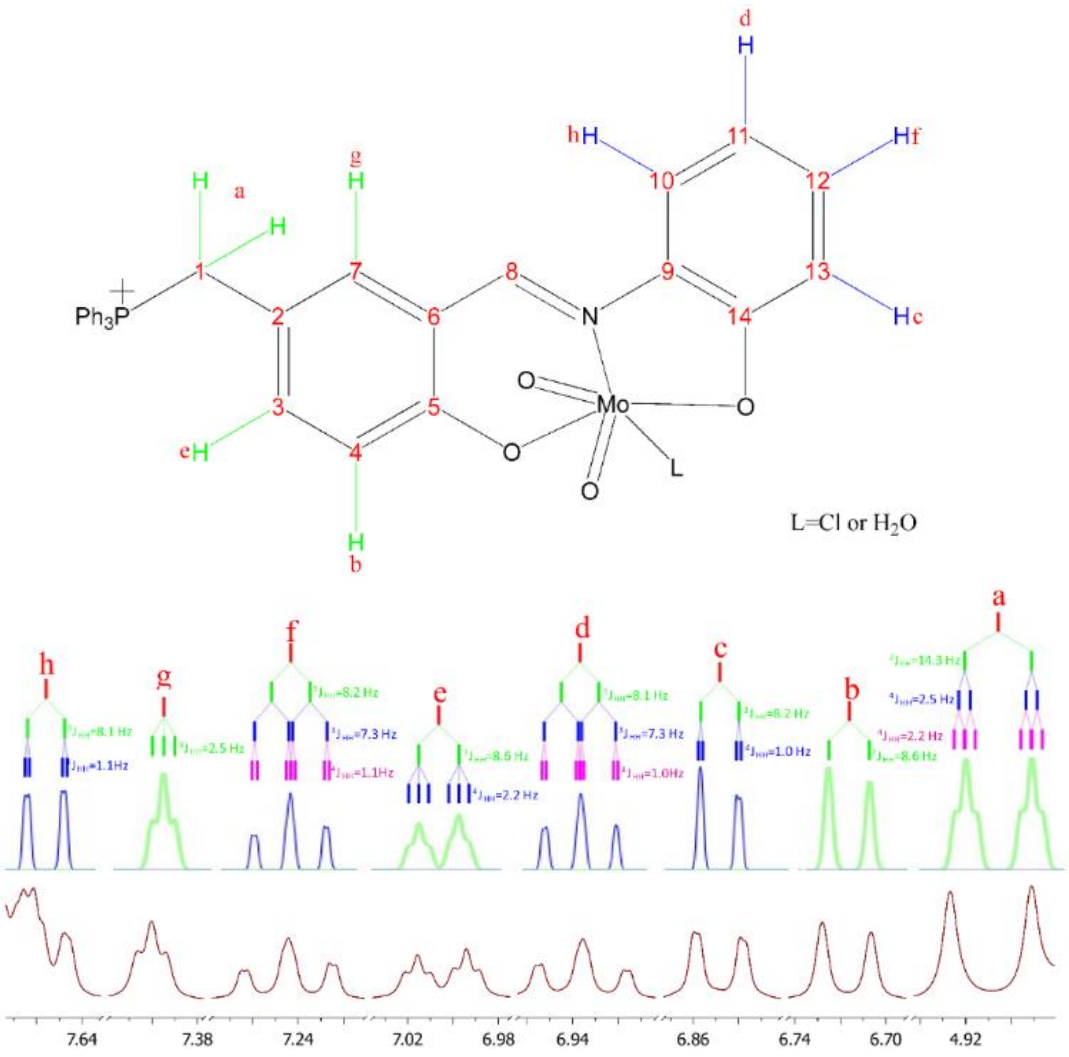

Figure 2. J-J coupling analysis of ^{1}H NMR spectrum of complex **4**

The ^{13}C NMR spectrum of complex **4** (Fig. S9) showed 18 sets of resonances. In order to assign these signals, ^{1}H-^{13}C HSQC and ^{1}H-^{13}C HMBC analyses were performed (Fig. S14-S17). According to the ^{1}H-^{13}C HSQC and ^{1}H-^{13}C HMBC NMR spectra, the resonances of carbon atoms of ipso, ortho, meta and para positions of phenyl phosphonium rings were appeared as a doublet resonance at δ= 118.9 ($^{1}J_{PC}$=85.9 Hz), 131.5 ($^{2}J_{PC}$=12.5 Hz), 135.4 ($^{3}J_{PC}$=9.7 Hz), and 136.5 ($^{4}J_{PC}$=3.0 Hz) ppm, respectively. The doublet resonance in the aliphatic region (29.7 ppm) is represented to the benzylic carbon atom with $^{1}J_{PC}$=48.1 Hz. The correlation between the singlet signal at 156.8 ppm and aldimine hydrogen in ^{1}H-^{13}C HSQC shows that this resonance is related to imine carbon. According to Fig S.15, four singlet resonances at δ=117.0, 118.6, 122.3 and 131.8 ppm are correlated to ((h)), ((c)), ((d)) and ((f)) hydrogen atoms respectively, and they are assigned to ((10)), ((13)), ((11)) and ((12)) carbon atoms, respectively (carbon labeling is illustrated in Fig. 2). Three doublet signals at δ= 120.7 ($^{4}J_{PC}$=2.8 Hz), 138.4 ($^{3}J_{PC}$=4.1 Hz) and 138.4 ($^{3}J_{PC}$=5.9 Hz) ppm have a correlation with ((b)), ((e)) and ((g)) hydrogen atoms, respectively, and they are

assigned to ((4)), ((3)) and ((7)) carbon atoms, respectively. Due to the relatively large coupling constant of doublet signal at δ = 121.1 ppm ($^{2}J_{PC}$=8.5 Hz), this signal is represented to the carbon atom 2. Two phenolic carbons ((5)) and ((14)) resonances were appeared at δ = 163.6 and 161.9 ppm as a doublet ($^{5}J_{PC}$= 3.2 Hz) and a singlet signals, respectively. At last, two other signals at δ =136.7 (singlet) and 123.8 (doublet, $^{4}J_{PC}$=2.9 Hz) are assigned to carbon nucleus ((6)) and ((9)), respectively.

The ^{31}P NMR spectrum of complex 4 (Fig. S10) shows one signal at δ= 22.6 ppm, illustrating that just one type of phosphorus atom existed in the structure with the chemical shift in the range of phosphonium salt chemical shifts [25]. The expansion of the ^{31}P NMR spectrum shows satellite, through coupling with ^{13}C nucleus (Fig. S11)

The FT-IR spectrum of complex 4 shows three important signals in 1612, 900 and 845 cm^{-1}, characterized as stretching vibrational mode of imine band and molybdenum dioxo symmetrical and unsymmetrical stretching vibrational modes, respectively (Fig. S18) [4d, 26].

3.2. X-ray crystal characterization

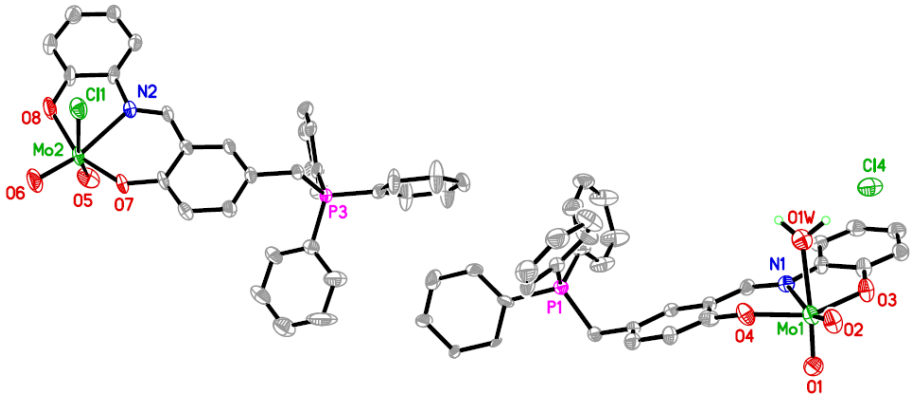

Figure 3. The ORTEP of complex **4** with selected atoms numbering and ellipsoids probability at 40%. The hydrogen atoms (except for coordinated aqua ligand) were omitted for clarity and only the major part was shown.

The ORTEP view of the complexes is shown in Fig. 3. Details of the data collection and refinement parameters are summarized in Table 1. Selected bond lengths and angles are summarized in Table 2. The hydrogen bonding parameters are summarized in Table 3.

Table 1. Crystal data and structure refinement for complex **4**

Empirical formula	C64 H52 Cl2 Mo2 N2 O9 P2
Formula weight	1317.80
Temperature (K)	150(2)
Wavelength (Å)	1.54184
Crystal system	Hexagonal
Space group	$P6_5$
Unit cell dimensions	
a (Å)	12.2043(3)
b (Å)	12.2043(3)
c (Å)	76.2069(17)
α (deg)	90
β (deg)	90
γ (deg)	120
Volume ($Å^3$)	9829.9(5)
Z	6
Density (calculated) (Mg/m^3)	1.336
Absorption coefficient (mm^{-1})	4.780
F(000)	4020
Crystal size (mm)	0.13 × 0.11 × 0.05
Theta range for data collection (deg)	4.2 to 72.091
Index ranges	-14≤h≤13, -14≤k≤13, -59≤l≤93
Reflections collected	30889
Independent reflections	8782 [R(int) = 0.065]
Completeness to theta = 67.684°	99.9 %
Refinement method	Full-matrix least-squares on F^2
Data / restraints / parameters	8782 / 566 / 813
Goodness-of-fit on F^2	1.019
Final R indices [I > 2 σ(I)]	R1 = 0.0510, wR2 = 0.1174
R indices (all data)	R1 = 0.0619, wR2 = 0.1186
Absolute structure parameter	-0.014(9)
Largest diff. peak and hole	0.43 and -0.44 e. $Å^{-3}$

The asymmetric unit of the complex comprises two chemically and crystallographically different molybdenum Schiff base complexes. In one of them, M1, the dianionic ONO, two oxo, and the chlorido ligands are coordinated to the molybdenum center in a distorted octahedral geometry; the compound being neutral. In the other one the dianionic ONO, two oxo, and aqua ligands are coordinated to molybdenum center. As this complex is cationic, there is a chloride anion for charge balance.

Table 2. Selected bond lengths and angles

N1–Mo1	2.293(7)
N2–Mo2	2.302(7)
O1–Mo1	1.677(9)
O2–Mo1	1.681(6)
O3–Mo1	1.979(7)
O4–Mo1	1.932(6)
O5–Mo2	1.660(9)
Cl1–Mo2	2.569(4)
O6–Mo2	1.679(10)
O7–Mo2	1.944(7)

Due to the strong π-donor character of the terminal oxo group, the Mo2–Cl1 [2.569(4) Å] and Mo1–O1w [2.278(8) Å] bonds are longer than the normal lengths. These are in agreement with the similar complexes reported previously [27]. The crystal packing, Fig. 4, is stabilized by the intermolecular O–H···Cl, C–H···O, and C–H···Cl interactions.

Table 3. Hydrogen bonds parameters for complex **4**

D–H···A	D–H	H...A	D...A	DHA
O1W–H1WB···Cl4[a]	0.93	2.30	3.061(7)	139
C14–H14A···Cl1[b]	0.97	2.70	3.588(9)	152
C14–H14B···Cl4[b]	0.97	2.77	3.716(8)	164
C16–H16···Cl4[b]	0.93	2.74	3.627(16)	158
C22–H22···O5[c]	0.93	2.53	3.12(2)	121
C46–H46A···O1[d]	0.97	2.32	3.262(11)	164
C49–H49A···O3[e]	0.93	2.39	3.151(11)	139
C54–H54A···Cl1[f]	0.93	2.58	3.364(9)	143
C54–H54A···O6A[f]	0.93	2.21	2.86(5)	125

(a)1+x,2+y,z+1; (b) x,1+y,z; (c) 1+x, 1+y, z; (d) x,-1+y, z; (e) -1+x,-2+y, z; (f) y, 1-x+y, 1/6+z

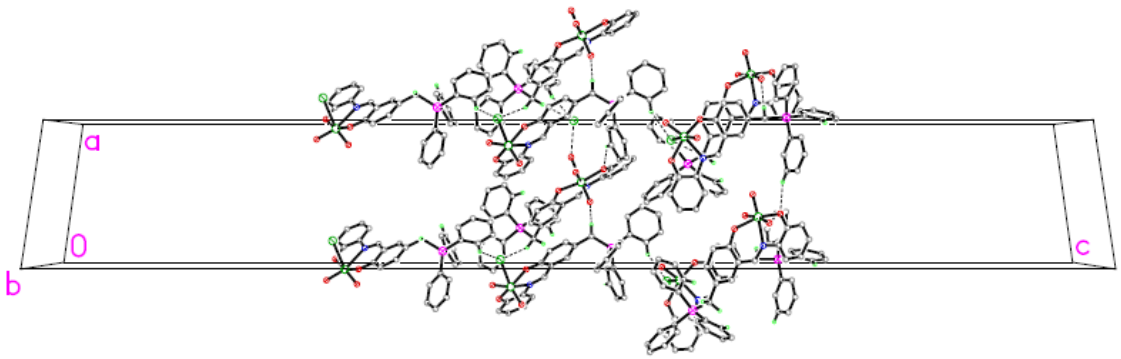

Figure 4. The crystal packing of the complex **4** viewed down the b-axis, showing the connection of molecules through the intermolecular interactions (dashed line) along the a-axis.

3.3. Electronic structure

Two different complexes (**4a** and **4b**) were observed in the X-ray single crystal analysis. These two complexes are similar to hydrate isomerism derived through the displacement of aqua with the chlorido ligand. Hence full geometry optimization was done for both complexes. After optimization, the vibrational frequency showed both complexes were in the minimum energy level. Optimized structures of 4a and 4b are illustrated in Fig. 5. (Details of optimized bonds lengths and angles are alleged in table S1-S4 in supporting information).

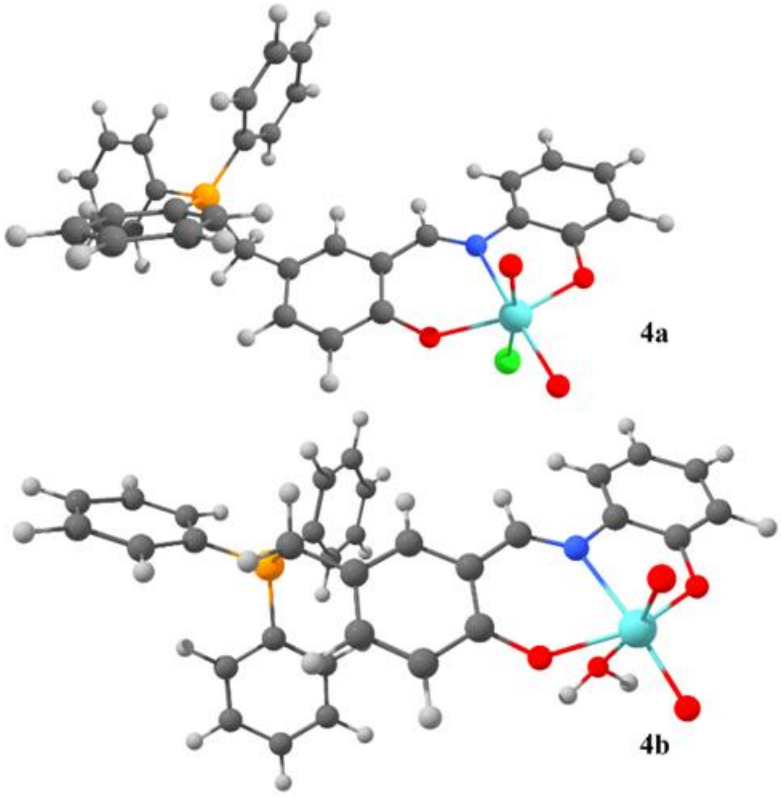

Figure 5. Optimized structure of complex **4a** and **4b**

The results obtained from the DFT calculations show that angles and length of the chemical bonds have an acceptable agreement with the values obtained from the crystallography experiment. The contour map of frontier molecular orbitals of **4a** and **4b** are illustrated in Fig. 6, Fig. S19 and S20, and the energy and composition of them are shown in table S5 and S6 respectively. In overall, it is very important to understand the nature of frontier molecular orbitals, because they play a critical role in both chemical activity and electronic transition of the complexes. These data confirm that both complexes have a closed-shell structure, and also the large energy gap between HOMO and LUMO illustrates the low chemical activity and kinetic stability of both complexes [28]. According to Fig. 6, and table S5 and S6, for complex **4a** and **4b**, the HOMO orbitals are

distributed over the ligand (about 91 % on benzyl and aminophenol rings and imine group for 4a and more than 95% on benzyl and aminophenol rings and imine group for 4b) and only 1% of HOMO is located on the metal center. Whereas, LUMO has a significant contribution to the metal center (41% for 4a and 38% for 4b). These calculations indicate that a nucleophillic attack occurs on the metal center.

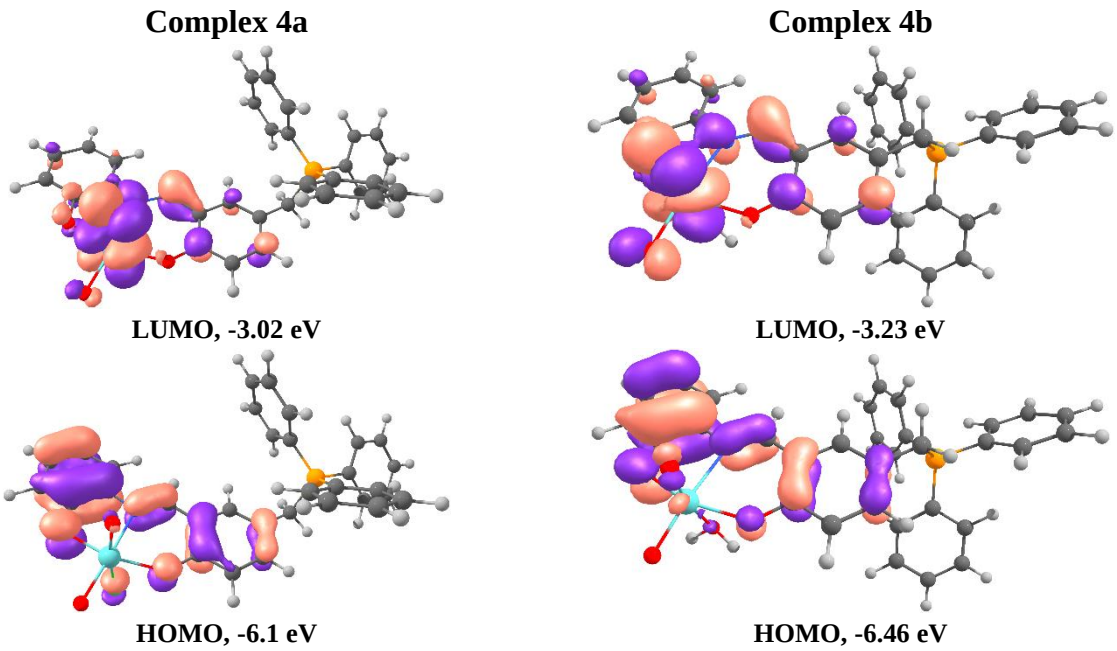

Figure 6. Contour map and energy of the HOMO and LOMO orbitals of complex **4a** and **4b**

Experimental absorption spectrum of complex **4** and simulated absorption spectra of **4a** and **4b** are compared in Fig. 7.

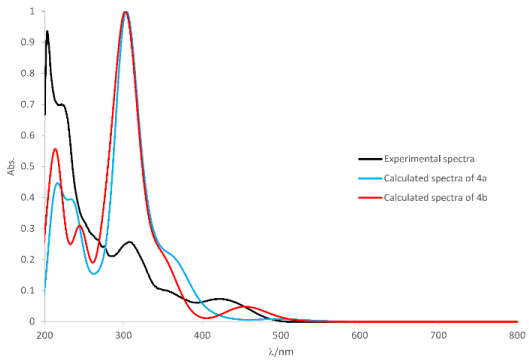

Figure 7. Experimental and simulated absorption spectra of complex **4**

The selected TD-DFT calculated spectra parameter of complex **4a** and **4b** along with their assignment are summarized in Table 4 (Full parameter of simulated absorption spectra are shown in Table S7 and Table S8 in supporting information). As it is observed in Table 4, each of the

electronic spectrum bands is assigned to a special transition. More than 97% of the transition band in 440 nm relates to transitions from the HOMO orbitals to LUMO and according to the nature of HOMO and LUMO orbitals, this transition can be assigned as LMCT transition.

Table 4. Selected TD-DFT calculated spectra parameter of complex 4a and 4b

λ/nm	*f*	**assignment**	λ/nm	*f*	**assignment**
Com. 4a			**Com. 4b**		
497	0.005	H→L (98%)	454	0.026	H→L (97%)
376	0.030	H-1→L (74%), H→L+2 (15%), H→L+3 (7%)	349	0.074	H→L+2 (45%), H-1→L (44%)
362	0.084	H-1→L (18%), H→L+2 (62%), H→L+3 (9%)	326	0.036	H-1→L+1 (56%), H→L+3 (24%), H-2→L (13%)
330	0.091	H-3→L (28%), H→L+3 (55%), H→L+2 (8%)	320	0.054	H-1→L+1 (40%), H→L+3 (31%), H-2→L (20%)
309	0.091	H-5→L (68%), H-3→L (8%)	303	0.432	H-2→L (60%), H→L+3 (22%), H→L+2 (8%)
304	0.200	H-3→L (15%), H-2→L (22%), H-1→L+2 (29%), H→L+3 (11%), H-1→L+3 (9%)	290	0.101	H-1→L+2 (81%), H-1→L+3 (9%)
300	0.241	H-3→L+1 (12%), H-2→L (11%), H-2→L+1 (13%), H-1→L+2 (35%), H-3→L (6%)	279	0.070	H-2→L+1 (90%)
299	0.067	H-3→L+1 (29%), H-2→L+1 (33%), H-1→L+2 (15%)	275	0.060	H-1→L+3 (78%), H-1→L+2 (7%)
265	0.036	H→L+5 (83%), H→L+6 (9%)	245	0.066	H-2→L+3 (84%)
240	0.028	H-1→L+4 (88%)	244	0.061	H→L+5 (82%), H→L+6 (7%)
239	0.090	H-3→L+3 (42%), H-2→L+3 (34%), H-4→L+3 (6%)	226	0.050	H-1→L+4 (84%), H-2→L+4 (7%)
234	0.030	H-9→L (14%), H-5→L+2 (31%), H-15→L (8%), H-14→L (8%), H-6→L (7%)	217	0.065	H-1→L+5 (39%), H-4→L+1 (35%)
218	0.072	H-12→L (14%), H-11→L (12%), H→L+8 (45%), H-10→L (6%)	215	0.075	H→L+7 (51%), H-11→L+1 (16%), H-10→L+1 (6%), H→L+8 (6%)
215	0.046	H-14→L+1 (22%), H-13→L+1 (24%), H-13→L+2 (12%), H→L+8 (12%), H-13→L+3 (7%)	214	0.041	H→L+7 (32%), H-11→L+1 (23%), H-10→L+1 (10%), H-6→L+1 (6%)
209	0.070	H-15→L+1 (21%), H-13→L+2 (44%), H-14→L+2 (9%)	209	0.036	H→L+8 (19%), H-10→L+2 (15%), H-11→L+2 (14%), H-1→L+6 (14%), H-4→L+2 (13%)
208	0.033	H→L+9 (25%), H→L+10 (59%)	201	0.034	H-3→L+3 (38%), H-6→L+2 (30%)

H: HOMO; L: LUMO

3.4. Catalytic studies

To evaluate the catalytic capability of **4** in epoxidation of olefins in water, the catalyst, cyclooctene and TBHP with the molar ratio of 1:500:1000 were selected as a primitive model in 0.5 mL of water and 80 °C (Table 5, entry 11), and the yield was 87.8%. In order to clarify the role of catalyst, a reaction was investigated under mentioned conditions in the absence of the catalyst and the yield was 17%, which confirms the catalyst's potential. According to entries, 1-4 (Table 5) the optimum ratio for substrate and TBHP was 1:2 (entry 4). Due to the fact that few cases have been reported to use water as the solvent of catalytic epoxidation, and the catalyst introduced by authors has shown high activity in water, only water was evaluated as the solvent of the catalytic system. In this regard, among different volumes of solvent, 0.5 mL was the most efficient volume (entry 6). In addition, by examination of different catalyst loadings, 0.2 mol% was chosen as the optimum loading amount (entry 12). In the following, the selected initial temperature (80 °C) was the most efficient temperature. During all these processes epoxy cyclooctane was the only observed reaction product. After optimization of the catalytic system condition, reaction progress was monitored based on the time (Fig. 8). Almost after 5 h, no notable progress was observed in the yield.

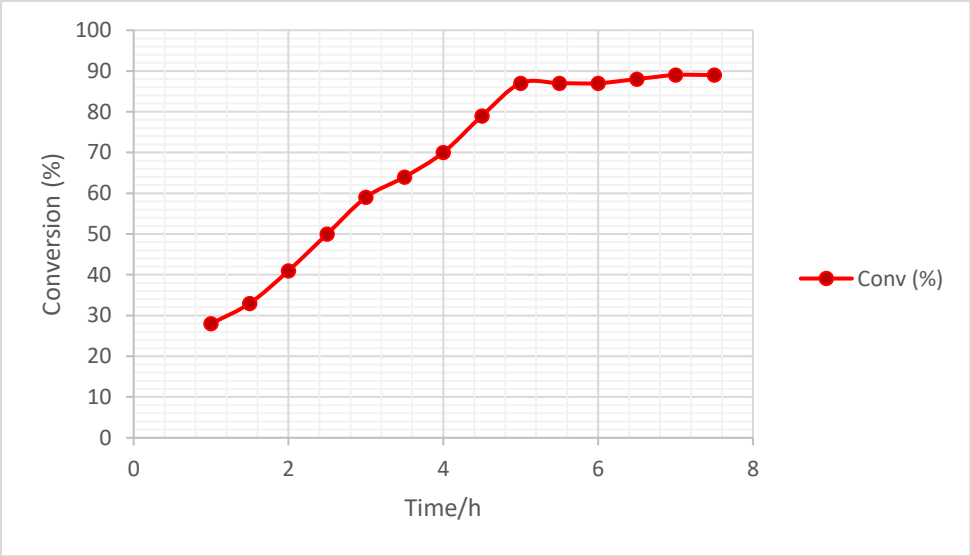

Figure 8. Reaction profile of the epoxidation of cyclooctene in optimized condition for **4**

According to mechanisms described in different publications [6h, 29], cessation of the reaction after 5 h can be due to the coordination of t-BuOH (resulted from TBHP) to the central molybdenum. To validate the catalytic reaction results, 10 times scaled-up catalytic reaction was investigated under the optimum condition and the conversion obtained 93.4% with 100% selectivity to epoxide. This observation shows that large scale experiment gives better output, compared with small scale catalytic reaction.

Table 5. Effect of the catalyst amount, TBHP amount, water amount and Temperature on the epoxidation of cyclooctene using **4** as a catalyst

Entry	Mol% Cat	TBHP (mmol)	Solv (mL)	Temp (°C)	Conv%[a]	Sel%	TON[b]
1	0.1	0	1	80	0	100	0
2	0.1	1	1	80	13.6	100	136
3	0.1	1.5	1	80	50.8	100	508
4	0.1	2	1	80	74.4	100	744
5	0.1	2	0	80	39.8	100	398
6	0.1	2	0.5	80	81.2	100	812
7	0.1	2	1.5	80	61.8	100	618
8	0.1	2	2	80	43.5	100	435
9	-	2	0.5	80	17.4	100	-
10	0.05	2	0.5	80	73.5	100	1470
11	0.15	2	0.5	80	84.6	100	564
12	**0.2**	**2**	**0.5**	**80**	**87.8**	**100**	**439**
13	0.3	2	0.5	80	88.2	100	294
14	0.4	2	0.5	80	88.5	100	221
15	0.5	2	0.5	80	89.1	100	178
16	0.2	2	0.5	r.t.	3.6	100	18
17	0.2	2	0.5	50	9.4	100	47
18	0.2	2	0.5	60	42.1	100	210
19	0.2	2	0.5	70	72.6	100	363
20	0.2	2	0.5	Reflux	88.4	100	442

[a] Time: 5 h. Cyclooctene: 1 mmol. Solvent: water. Conversions are calculated by GC based on starting alkenes
[b] Turnover number= moles of desired product formed/moles of catalyst

The catalytic results are exhibited for various olefins in Table 6. As it is illustrated in entry 1 and 2, the cyclic alkene with bigger ring undergoes more conversion and selectivity. Also, for cyclic alkenes with the same number of ring carbons, the one with more group on C=C shows more conversion and selectivity (entries 2, 3). In opposition to alkenes inside the ring, for alkenes outside the ring, the one with fewer groups on C=C endures less conversion, but more selectivity (entries 4, 5). Also for stilbenes, the *Trans* structure led the reaction to more yield and less selectivity in comparison with *cis* structure (entries 7, 8). In the terminal linear olefins, shorter chains are dominant in both conversion and selectivity against longer chains (entries 9, 10) [4d, 30]. Additionally, in the linear olefins, the catalyst showed more activity and fewer side products for internal C=C (entries 11, 12). Among all the substrates, the lowest yield was obtained for indene (entry 6).

Table 6. Epoxidation of various olefins using TBHP and **4**

Entry	Substrate	Conv%[a]	Sel%	TON[b]
1	cyclooctene	87.8	100	439
2	cyclohexene	63.2	91	316
3	1-methylcyclohexene	86.3	100	431
4	styrene	31.2	14	156
5	α-methylstyrene	23.5	28	117
6	Indene	8	20	40
7	Cis-stilbene	41.3	73	206
8	Trans-stilbene	56.7	57	283
9	1-heptene	61.7	85	308
10	1-octene	36	59	180
11	Trans-2-octene	64.5	89	322

[a] Reaction condition: 0.2 mol% cat, 1 mmol olefin, 2 mmol TBHP, 0.5 mL water solvent, Time 5 h and temperature 80 °C. Conversions are calculated by GC based on starting alkene.
[b] Turnover number= moles of desired product formed/moles of catalyst

4. Conclusion

In summary, a new Mo(VI) Schiff base cationic complex was synthesized and fully characterized. The asymmetric unit of the complex comprises two chemically and crystallographically different molybdenum Schiff base complexes. Therefore, DFT studies were performed for both complexes and the nature of frontier molecular orbitals and electronic transitions were obtained. Afterward, a new protocol was defined for catalytic epoxidation of olefin through using this Mo(VI) complex as a homogeneous catalyst. In this protocol, 1,2-dichloroethane, a highly toxic solvent commonly used in the epoxidation reaction, is substituted with water as a green medium. The catalytic system showed good activity in water for epoxidation of varied olefins and the catalyst was successfully able to catalyze cyclooctene with a turnover number more than 1400.

5. Acknowledgments

M.B. acknowledges the research council of the Sharif University of Technology for the research funding of this work. RK is thankful to Bath University for a visiting lectureship. PRR is grateful to the Engineering and Physical Sciences Research Council (EPSRC) for continued funding (EP/K004956/1). The Università degli Studi di Perugia and MIUR are acknowledged for financial support to the project AMIS, through the program “Dipartimenti di Eccellenza - 2018-2022”.

Supporting Information

Crystallographic data for the structural analysis has been deposited in the Cambridge Crystallographic Data Centre, No. CCDC **1588804.** Experimental details, full characterization data, and Additional data for the computational study are available in the electronic supporting information.

References:

[1] a) K.A. Joergensen, Transition-metal-catalyzed epoxidations, Chem. Rev., 89 (1989) 431-458; b) G. Grigoropoulou, J.H. Clark, J.A. Elings, Recent developments on the epoxidation of alkenes using hydrogen peroxide as an oxidant, Green chem., 5 (2003) 1-7; c) N. Mizuno, K. Yamaguchi, K. Kamata, Epoxidation of olefins with hydrogen peroxide catalyzed by polyoxometalates, Coord. Chem. Rev., 249 (2005) 1944-1956; d) M. Amini, M.M. Haghdoost, M. Bagherzadeh, Monomeric and dimeric oxido–peroxido tungsten(VI) complexes in catalytic and stoichiometric epoxidation, Coord. Chem. Rev., 268 (2014) 83-100; e) Z. Guo, B. Liu, Q. Zhang, W. Deng, Y. Wang, Y. Yang, Recent advances in heterogeneous selective oxidation catalysis for sustainable chemistry, Chem. Soc. Rev., 43 (2014) 3480-3524.

[2] a) B.S. Lane, K. Burgess, Metal-Catalyzed Epoxidations of Alkenes with Hydrogen Peroxide, Chem. Rev., 103 (2003) 2457-2474; b) T.S.M. Oliveira, A.C. Gomes, A.D. Lopes, J.P. Lourenco, F.A. Almeida Paz, M. Pillinger, I.S. Goncalves, Dichlorodioxomolybdenum(vi) complexes bearing oxygen-donor ligands as olefin epoxidation catalysts, Dalton Trans., 44 (2015) 14139-14148; c) L. Tengfei, Z. Wei, C. Wei, M.H. N., S. Yu-Fei, Modular Polyoxometalate–Layered Double Hydroxides as Efficient Heterogeneous Sulfoxidation and Epoxidation Catalysts, ChemCatChem, 10 (2018) 188-197; d) P. Fatemeh, B. Abolfazl, E. Habibollah, Excellent alkene epoxidation catalytic activity of macrocyclic-based complex of dioxo-Mo(VI) on supermagnetic separable nanocatalyst, Appl. Organomet. Chem., 32 (2018) e3986; e) V.K. Chidara, S. Stadem, D.C. Webster, G. Du, Survey of several catalytic systems for the epoxidation of a biobased ester sucrose soyate, Catal. Commun., 111 (2018) 31-35; f) M. Fadhli, I. Khedher, J.M. Fraile, Enantioselective epoxidation of styrene with TBHP catalyzed by bis(oxazoline)–vanadyl–laponite materials, Catal. Commun., 117 (2018) 90-93.

[3] a) A. Dupé, M.K. Hossain, J.A. Schachner, F. Belaj, A. Lehtonen, E. Nordlander, N.C. Mösch-Zanetti, Dioxomolybdenum(VI) and -tungsten(VI) Complexes with Multidentate Aminobisphenol Ligands as Catalysts for Olefin Epoxidation, Eur. J. Inorg. Chem., 2015 (2015) 3572-3579; b) A.E. Kuznetsov, Y.V. Geletii, C.L. Hill, K. Morokuma, D.G. Musaev, Mechanism of the Divanadium-Substituted Polyoxotungstate [γ-1,2-H2SiV2W10O40]4− Catalyzed Olefin Epoxidation by H2O2: A Computational Study, Inorg. Chem., 48 (2009) 1871-1878; c) D. Betz, W.A. Herrmann, F.E. Kühn, Epoxidation in ionic liquids: A comparison of rhenium(VII) and molybdenum(VI) catalysts, J. Organomet. Chem., 694 (2009) 3320-3324; d) M. Cokoja, M. Markiewicz, S. Stolte, F.E. Kühn, Toxicity Assessment of Molecular Rhenium(VII) Epoxidation Catalysts, in: Encyclopedia of Inorganic and Bioinorganic Chemistry, John Wiley & Sons, Ltd, 2011; e) A. Castro, J.C. Alonso, A.A. Valente, P. Neves, P. Brandão, V. Félix, P. Ferreira, Nanostructured Dioxomolybdenum(VI) Catalyst for the Liquid-Phase Epoxidation of Olefins, Eur. J. Inorg. Chem., 2010 (2010) 1405-1412; f) A. Jimtaisong, R.L. Luck, Synthesis and Catalytic Epoxidation Activity with TBHP and H2O2 of Dioxo-, Oxoperoxo-, and Oxodiperoxo Molybdenum(VI) and Tungsten(VI) Compounds Containing Monodentate or Bidentate Phosphine Oxide Ligands: Crystal Structures of WCl2(O)2(OPMePh2)2, WCl2(O)(O2)(OPMePh2)2, MoCl2(O)2dppmO2·C4H10O, WCl2(O)2dppmO2, Mo(O)(O2)2dppmO2, and W(O)(O2)2dppmO2, Inorg. Chem., 45 (2006) 10391-10402; g) A.O. Chong, K.B. Sharpless, Mechanism of the molybdenum and vanadium catalyzed epoxidation of olefins by alkyl hydroperoxides, J. Org. Chem., 42 (1977) 1587-1590; h) W. Zhang, H. Yamamoto, Vanadium-Catalyzed Asymmetric Epoxidation of Homoallylic Alcohols, J. Am. Chem. Soc., 129 (2007) 286-287; i) Z. Bourhani, A.V. Malkov, Ligand-accelerated vanadium-catalysed epoxidation in water, Chem. Commun., (2005) 4592-4594; j) J.-M. Bregeault, Transition-metal complexes for liquid-phase catalytic oxidation: some aspects of industrial reactions and of emerging technologies, Dalton Trans., (2003) 3289-3302; k) A.M. Al-Ajlouni, J.H. Espenson, Kinetics and Mechanism of the Epoxidation of Alkyl-Substituted Alkenes by Hydrogen Peroxide, Catalyzed by Methylrhenium Trioxide, J. Org. Chem., 61 (1996) 3969-3976; l) V. Vrdoljak, J. Pisk, B. Prugovečki, D. Agustin, P. Novak, D. Matković-Čalogović, Dioxotungsten(vi) complexes with isoniazid-related hydrazones as (pre)catalysts for olefin epoxidation: solvent and ligand substituent effects, RSC Adv., 6 (2016) 36384-36393.

[4] a) M. Amini, M.M. Haghdoost, M. Bagherzadeh, Oxido-peroxido molybdenum(VI) complexes in catalytic and stoichiometric oxidations, Coord. Chem. Rev., 257 (2013) 1093-1121; b) C. Müller, N. Grover, M. Cokoja, F.E. Kühn, Chapter Two - Homogeneous Catalytic Olefin Epoxidation with Molybdenum Complexes, in: R. van Eldik, C.D. Hubbard (Eds.) Adv. Inorg. Chem., Academic Press, 2013, pp. 33-83; c) M. Cindric, G. Pavlovic, R. Katava, D. Agustin, Towards a global greener process: from solvent-less synthesis of molybdenum(vi) ONO Schiff base complexes to catalyzed olefin epoxidation under organic-solvent-free conditions, New J. Chem., 41 (2017) 594-602; d) M. Bagherzadeh, S. Ataie, H. Mahmoudi, J. Janczak, Synthesis, structure characterization and study of a new molybdenum Schiff base complex as an epoxidation catalyst with very high turnover numbers, Inorg. Chem. Commun., 84 (2017) 63-67; e) D. Cvijanović, J. Pisk, G. Pavlović, D. Šišak-Jung, D. Matković-Čalogović, M. Cindrić, D. Agustin, V. Vrdoljak, Discrete mononuclear and dinuclear compounds containing a MoO22+ core and 4-aminobenzhydrazone ligands: synthesis, structure and organic-solvent-free epoxidation activity, New J. Chem., 43 (2019) 1791-1802; f) J. Pisk, B. Prugovečki, D. Matković-Čalogović, T. Jednačak, P. Novak, D. Agustin, V. Vrdoljak, Pyridoxal hydrazonato molybdenum(vi) complexes: assembly, structure and epoxidation (pre)catalyst testing under solvent-free conditions, RSC Adv., 4 (2014) 39000-39010; g) D. Julião, A.C. Gomes, L. Cunha-Silva, M. Pillinger, A.D. Lopes, R. Valença, J.C. Ribeiro, I.S. Gonçalves, S.S. Balula, Dichlorodioxomolybdenum(VI) complexes bearing oxygen-donor ligands as catalysts for oxidative desulfurization of simulated and real diesel, Catal. Commun., (2019) 105704.

[5] G.P. Chiusoli, P.M. Maitlis, R.S.o. Chemistry, Metal-catalysis in Industrial Organic Processes, RSC Publishing, 2008.

[6] a) N. Zwettler, N. Grover, F. Belaj, K. Kirchner, N.C. Mösch-Zanetti, Activation of Molecular Oxygen by a Molybdenum(IV) Imido Compound, Inorg. Chem., 56 (2017) 10147-10150; b) E.I. Stiefel, W.E. Newton, G.D. Watt, K.L. Hadfield, W.A. Bulen, Molybdoenzymes: The Role of Electrons, Protons, and Dihydrogen, in: Bioinorganic Chemistry—II, AMERICAN CHEMICAL SOCIETY, 1977, pp. 353-388; c) L. Banci, Metallomics and the Cell, Springer Netherlands, 2013; d) A. Magalon, J.G. Fedor, A. Walburger, J.H. Weiner, Molybdenum enzymes in bacteria and their maturation, Coord. Chem. Rev., 255 (2011) 1159-1178; e) R. Abdolreza, S. Iran, M. Niaz, S.E. Helen, Synthesis, Crystal Structure, and Catalytic Properties of Novel Dioxidomolybdenum(VI) Complexes with Tridentate Schiff Base Ligands in the Biomimetic and Highly Selective Oxygenation of Alkenes and Sulfides, Eur. J. Inorg. Chem., 2010 (2010) 799-806; f) D. Eierhoff, W.C. Tung, A. Hammerschmidt, B. Krebs, Molybdenum complexes with O,N,S donor ligands as models for active sites in oxotransferases and hydroxylases, Inorg. Chim. Acta, 362 (2009) 915-928; g) M. Bagherzadeh, L. Tahsini, R. Latifi, A. Ellern, L.K. Woo, Synthesis, crystal structure and catalytic activity of a novel Mo(VI)–oxazoline complex in highly efficient oxidation of sulfides to sulfoxides by urea hydrogen peroxide, Inorg. Chim. Acta, 361 (2008) 2019-2024; h) M. Bagherzadeh, R. Latifi, L. Tahsini, V. Amani, A. Ellern, L. Keith Woo, Synthesis, characterization and crystal structure of a dioxomolybdenum(VI) complex with a N,O type bidentate Schiff base ligand as a catalyst for homogeneous oxidation of olefins, Polyhedron, 28 (2009) 2517-2521.

[7] a) N.K. Ngan, K.M. Lo, C.S.R. Wong, Synthesis, structure studies and electrochemistry of molybdenum(VI) Schiff base complexes in the presence of different donor solvent molecules, Polyhedron, 30 (2011) 2922-2932; b) T. Fang, H.-X. Lu, J.-X. Zhao, S.-Z. Zhan, Synthesis and studies of a molecular molybdenum–Schiff base electrocatalyst for generating hydrogen from organic acid or water, Inorg. Chem. Commun., 51 (2015) 66-70; c) H. Amiri Rudbari, M. Khorshidifard, B. Askari, N. Habibi, G. Bruno, New asymmetric Schiff base ligand derived from allylamine and 2,3-dihydroxybenzaldehyde and its molybdenum(VI) complex: Synthesis, characterization, crystal structures, computational studies and antibacterial activity together with synergistic effect against Pseudomonas aeroginosa PTTC 1570, Polyhedron, 100 (2015) 180-191; d) A.Z. Wail, A.H.A.A. Salih, K. Mosab, Synthesis and antioxidant activities of Schiff bases and their complexes: a review, Appl. Organomet. Chem., 30 (2016) 810-817; e) M.M. Haghdoost, N. Zwettler, G. Golbaghi, F. Belaj, M. Bagherzadeh, J.A. Schachner, N.C. Mösch-Zanetti,

Diastereoselective synthesis and catalytic activity of two chiral cis-dioxido molybdenum (VI) complexes, Eur. J. Inorg. Chem; f) M.E. Judmaier, C. Holzer, M. Volpe, N.C. Mösch-Zanetti, Molybdenum(VI) Dioxo Complexes Employing Schiff Base Ligands with an Intramolecular Donor for Highly Selective Olefin Epoxidation, Inorg. Chem., 51 (2012) 9956-9966.
[8] Q. Liu, Y. Yang, W. Hao, Z. Xu, L. Zhu, Synthesis, Characterization and Biological Activity of Cis-Dioxomolybdenum(VI) Schiff base Complex [MoO2(L)2], IERI Procedia, 5 (2013) 178-183.
[9] a) W. De Soete, C. Jimenez-Gonzalez, P. Dahlin, J. Dewulf, Challenges and recommendations for environmental sustainability assessments of pharmaceutical products in the healthcare sector, Green chem., 19 (2017) 3493-3509; b) C.J. Clarke, W.-C. Tu, O. Levers, A. Bröhl, J.P. Hallett, Green and Sustainable Solvents in Chemical Processes, Chem. Rev., 118 (2018) 747-800.
[10] a) B.C. Ranu, A. Saha, R. Dey, Using more environmentally friendly solvents and benign catalysts in performing conventional organic reactions, Current opinion in drug discovery & development, 13 (2010) 658-668; b) T. Welton, Solvents and sustainable chemistry, in: Proc. R. Soc. A, The Royal Society, 2015, pp. 20150502.
[11] a) R. Breslow, The Principles of and Reasons for Using Water as a Solvent for Green Chemistry, in: Handbook of Green Chemistry, Wiley-VCH Verlag GmbH & Co. KGaA, 2010; b) B. Karimi, F. Mansouri, H. Vali, A highly water-dispersible/magnetically separable palladium catalyst based on a Fe3O4@SiO2 anchored TEG-imidazolium ionic liquid for the Suzuki-Miyaura coupling reaction in water, Green chem., 16 (2014) 2587-2596; c) T. Kitanosono, K. Masuda, P. Xu, S. Kobayashi, Catalytic Organic Reactions in Water toward Sustainable Society, Chem. Rev., 118 (2018) 679-746.
[12] a) A. Rezaeifard, R. Haddad, M. Jafarpour, M. Hakimi, Catalytic Epoxidation Activity of Keplerate Polyoxomolybdate Nanoball toward Aqueous Suspension of Olefins under Mild Aerobic Conditions, J. Am. Chem. Soc., 135 (2013) 10036-10039; b) T. Omagari, A. Suzuki, M. Akita, M. Yoshizawa, Efficient Catalytic Epoxidation in Water by Axial N-Ligand-Free Mn-Porphyrins within a Micellar Capsule, J. Am. Chem. Soc., 138 (2016) 499-502; c) F. Ballistreri, C. Gangemi, A. Pappalardo, G. Tomaselli, R. Toscano, G. Trusso Sfrazzetto, (Salen)Mn(III) Catalyzed Asymmetric Epoxidation Reactions by Hydrogen Peroxide in Water: A Green Protocol, Int. J. Mol. Sci., 17 (2016) 1112; d) W. Zhao, C. Yang, Z. Cheng, Z. Zhang, A reusable catalytic system for sulfide oxidation and epoxidation of allylic alcohols in water catalyzed by poly(dimethyl diallyl) ammonium/polyoxometalate, Green chem., 18 (2016) 995-998; e) J.d.J. Cázares-Marinero, C. Przybylski, M. Salmain, Proteins as Macromolecular Ligands for Metal-Catalysed Asymmetric Transfer Hydrogenation of Ketones in Aqueous Medium, Eur. J. Inorg. Chem., 2018 (2018) 1383-1393; f) L. Wang, Y. Ye, V. Lykourinou, J. Yang, A. Angerhofer, Y. Zhao, L.J. Ming, Front Cover: Catalytic Cooperativity, Nuclearity, and O2/H2O2 Specificity of Multi-Copper(II) Complexes of Cyclen-Tethered Cyclotriphosphazene Ligands in Aqueous Media (Eur. J. Inorg. Chem. 42/2017), Eur. J. Inorg. Chem., 2017 (2017) 4884-4884.
[13] a) A.S. Dinca, N. Candu, S. Shova, F. Lloret, M. Julve, V.I. Parvulescu, M. Andruh, A new chiral dimanganese(iii) complex: synthesis, crystal structure, spectroscopic, magnetic, and catalytic properties, RSC Adv., 6 (2016) 86569-86574; b) R. Bikas, V. Lippolis, N. Noshiranzadeh, H. Farzaneh-Bonab, A.J. Blake, M. Siczek, H. Hosseini-Monfared, T. Lis, Electronic Effects of Aromatic Rings on the Catalytic Activity of Dioxidomolybdenum(VI)–Hydrazone Complexes, Eur. J. Inorg. Chem., 2017 (2017) 999-1006.
[14] a) S.J. Yang, W. Nam, Water-Soluble Iron Porphyrin Complex-Catalyzed Epoxidation of Olefins with Hydrogen Peroxide and tert-Butyl Hydroperoxide in Aqueous Solution, Inorg. Chem., 37 (1998) 606-607; b) T. Sakamoto, C. Pac, Selective epoxidation of olefins by hydrogen peroxide in water using a polyoxometalate catalyst supported on chemically modified hydrophobic mesoporous silica gel, Tetrahedron Lett., 41 (2000) 10009-10012; c) J. Li, F. Hu, X.-K. Xie, F. Liu, Z.-Z. Huang, Synthesis of new functionalized chiral ionic liquid and its organocatalytic asymmetric epoxidation in water, Catal. Commun., 11 (2009) 276-279; d) F. Fringuelli, R. Germani, F. Pizzo, G. Savelli, Epoxidation reaction with m-chloroperoxybenzoic acid in water, Tetrahedron Lett., 30 (1989) 1427-1428; e) J. Bernadou, A.-S. Fabiano,

A. Robert, B. Meunier, "Redox Tautomerism" in High-Valent Metal-oxo-aquo Complexes. Origin of the Oxygen Atom in Epoxidation Reactions Catalyzed by Water-Soluble Metalloporphyrins, J. Am. Chem. Soc., 116 (1994) 9375-9376.
[15] C. Li-Juan, M. Fu-Ming, L. Guang-Xing, Co(II) Schiff base complexes on silica by sol–gel method as heterogeneous catalysts for oxidative carbonylation of aniline, Catal. Commun., 10 (2009) 981-985.
[16] R.I. Kureshy, K.J. Prathap, T. Roy, N.C. Maity, N.-u.H. Khan, S.H.R. Abdi, H.C. Bajaj, Reusable Chiral Dicationic Chromium(III) Salen Catalysts for Aminolytic Kinetic Resolution of trans-Epoxides, Adv. Synth. Catal., 352 (2010) 3053-3060.
[17] M.M. Jones, A New Method of Preparing Some Acetylacetonate Complexes, J. Am. Chem. Soc., 81 (1959) 3188-3189.
[18] a) G.H. Cartledge, Equilibrium Between the Complexes of Tervalent Manganese with 2,4-Pentanedione, J. Am. Chem. Soc., 73 (1951) 4416-4419; b) W.L.F. Armarego, C. Chai, Purification of Laboratory Chemicals, Elsevier Science, 2009.
[19] A.M. Castillo, L. Patiny, J. Wist, Fast and accurate algorithm for the simulation of NMR spectra of large spin systems, J. Magn. Reson., 209 (2011) 123-130.
[20] R. Clark, J. Reid, The analytical calculation of absorption in multifaceted crystals, Acta Crystallogr. Sect. A: Found. Crystallogr., 51 (1995) 887-897.
[21] a) SuperNova Eos S2 System: Empirical absorption correction, CrysAlis-Software package, Oxford Diffraction Ltd, 2011; b) Z. Otwinowski, W. Minor, Processing of X-ray diffraction data collected in oscillation mode, Methods Enzymol., 276 (1997) 307-326.
[22] a) O.V. Dolomanov, L.J. Bourhis, R.J. Gildea, J.A. Howard, H. Puschmann, OLEX2: a complete structure solution, refinement and analysis program, J. Appl. Crystallogr., 42 (2009) 339-341; b) Agilent Technologies UK Ltd, Yarnton, Oxfordshire, England, AutoChem 2.0, in conjunction with OLEX2.
[23] G.M. Sheldrick, A short history of SHELX, Acta Crystallogr. Sect. A: Found. Crystallogr., 64 (2008) 112-122.
[24] A.L. Spek, Structure validation in chemical crystallography, Acta Crystallogr. Sect. D. Biol. Crystallogr., 65 (2009) 148-155.
[25] V.P. Balema, J.W. Wiench, M. Pruski, V.K. Pecharsky, Solvent-free mechanochemical synthesis of phosphonium salts, Chem. Commun., (2002) 724-725.
[26] a) W. Wang, J.-C. Daran, R. Poli, D. Agustin, OH-substituted tridentate ONO Schiff base ligands and related molybdenum(VI) complexes for solvent-free (ep)oxidation catalysis with TBHP as oxidant, J. Mol. Catal. A: Chem., 416 (2016) 117-126; b) M. Bagherzadeh, H. Mahmoudi, M. Amini, S. Gautam, K.H. Chae, SBA-15-Supported Copper (II) Complex: An Efficient Heterogeneous Catalyst for Azide-Alkyne Cycloaddition in Water, Sci. Iran, 25 (2018) 1335-1343.
[27] a) S. Gupta, S. Pal, A.K. Barik, S. Roy, A. Hazra, T.N. Mandal, R.J. Butcher, S.K. Kar, Molybdenum(VI) complexes of a few pyrimidine derived ligands and the study of metal mediated CN bond cleavage resulting in ligand transformation during complex formation, Polyhedron, 28 (2009) 711-720; b) V. Vrdoljak, B. Prugovecki, I. Pulic, M. Cigler, D. Sviben, J. Parlov Vukovic, P. Novak, D. Matkovic-Calogovic, M. Cindric, Dioxidomolybdenum(vi) complexes with isoniazid-related hydrazones: solution-based, mechanochemical and UV-light assisted deprotonation, New J. Chem., 39 (2015) 7322-7332.
[28] J.-i. Aihara, Reduced HOMO−LUMO Gap as an Index of Kinetic Stability for Polycyclic Aromatic Hydrocarbons, J. Phys. Chem. A, 103 (1999) 7487-7495.
[29] a) A. Zarnegaryan, M. Moghadam, S. Tangestaninejad, V. Mirkhani, I. Mohammdpoor-Baltork, A graphene oxide immobilized Cu(ii) complex of 1,2-bis(4-aminophenylthio)ethane: an efficient catalyst for epoxidation of olefins with tert-butyl hydroperoxide, New J. Chem., 40 (2016) 2280-2286; b) M. Mirzaee, B. Bahramian, A. Amoli, Schiff base-functionalized boehmite nanoparticle-supported molybdenum and vanadium complexes: efficient catalysts for the epoxidation of alkenes, Appl. Organomet. Chem., 29 (2015) 593-600.

[30] M. Bagherzadeh, M. Zare, T. Salemnoush, S. Özkar, S. Akbayrak, Immobilization of dioxomolybdenum(VI) complex bearing salicylidene 2-picoloyl hydrazone on chloropropyl functionalized SBA-15: A highly active, selective and reusable catalyst in olefin epoxidation, Appl. Catal., A, 475 (2014) 55-62.